Toward Better Antibiotics: Crystallographic Studies of a Novel Class of DD-Peptidase/β-Lactamase Inhibitors†

Nicholas R. Silvaggi,‡ Kamaljit Kaur,§ S. A. Adediran,§ R. F. Pratt,*,§ and Judith A. Kelly*,‡

Department of Molecular and Cell Biology and Institute for Materials Science, University of Connecticut, Storrs, Connecticut 06269-3125, and Department of Chemistry, Wesleyan University, Middletown, Connecticut 06459-0180

Received February 25, 2004; Revised Manuscript Received March 31, 2004

ABSTRACT: β-Lactam antibiotics are vital weapons in the treatment of bacterial infections, but their future is under increasing threat from β-lactamases. These bacterial enzymes hydrolyze and inactivate β-lactam antibiotics, rendering the host cell resistant to the bactericidal effects of the drugs. Nevertheless, the bacterial D-alanyl-D-alanine transpeptidases (DD-peptidases), the killing targets of β-lactams, remain attractive targets for antibiotic compounds. Cyclic acyl phosph(on)ates have been developed and investigated as potential inhibitors of both transpeptidases and β-lactamases. The X-ray crystal structures of the complexes of the *Streptomyces* strain R61 DD-peptidase inhibited by a bicyclic [1-hydroxy-4,5-benzo-2,6-dioxaphosphorinanone(3)-1-oxide] and a monocyclic [1-hydroxy-4-phenyl-2,6-dioxaphosphorinanone(3)-1-oxide] acyl phosphate were determined to investigate the mode of action of these novel inhibitors. The structures show, first, that these inhibitors form covalent bonds with the active site serine residue of the enzyme and that the refractory complexes thus formed are phosphoryl-enzyme species rather than acyl enzymes. The complexes are long-lived largely because, after ring opening, the ligands adopt conformations that cannot directly recyclize, the latter a phenomenon previously observed with cyclic acyl phosph(on)ates. While the two inhibitors bind in nearly identical conformations, the phosphoryl-enzyme complex formed from the monocyclic compound is significantly less mobile than that formed from the bicyclic compound. Despite this difference, the complex with the bicyclic compound breaks down to regenerate free enzyme somewhat more slowly than that of the monocyclic. This may be because of steric problems associated with the reorientation of the larger bicyclic ligand required for reactivation. The structures are strikingly different in the orientation of the phosphoryl moiety from those generated using more specific phosph(on)ates. Models of the noncovalent complexes of the monocyclic compound with the R61 DD-peptidase and a structurally very similar class C β-lactamase suggest reasons why the former enzyme is phosphorylated by this compound, while the latter is acylated. Finally, this paper provides information that will help in the design of additional DD-peptidase inhibitors with the potential to serve as leads in the development of novel antibiotics.

β-Lactam antibiotics are bactericidal agents because they inhibit the enzymes responsible for the biosynthesis and maintenance of the bacterial cell wall (*1*−*6*). These enzymes are a class of penicillin-binding proteins (PBPs)[1] known as D-alanyl-D-alanine carboxypeptidase/transpeptidases (DD-peptidases). DD-peptidases catalyze the final step in cell-wall biosynthesis in which H_3N^+-X-D-alanyl-D-alanine peptides on individual peptidoglycan strands are cross-linked to form the rigid, meshlike structure of the bacterial cell wall. The cross-linking reaction begins with the noncovalent binding of the peptide portion of the peptidoglycan polymer to the DD-peptidase. A catalytic serine hydroxyl then attacks the carbonyl carbon of the penultimate D-alanine residue of the peptide to form a short-lived acyl enzyme intermediate, with the release of free D-alanine (reaction a in Scheme 1). The enzyme can then catalyze a transpeptidation reaction, where an amino group on a second strand of peptidoglycan attacks the ester of the acyl enzyme (reaction c in Scheme 1), cross-linking the two peptidoglycan strands and regenerating the free enzyme. Many DD-peptidases also possess carboxypeptidase activity, where water acts as the acceptor, yielding a shortened peptide product (reaction b in Scheme 1). The carboxypeptidase activity is thought to regulate the degree of cross-linking in the cell wall (*5*, *6*).

Penicillins and cephalosporins (β-lactams) react with PBPs because they mimic the D-alanyl-D-alanine motif of peptidoglycan. More specifically, the pyramidal nitrogen of the bicyclic β-lactam makes these drugs resemble the transition state in the reaction with peptide substrates (*7*, *8*). However, unlike peptide substrates, β-lactam antibiotics form extremely long-lived acyl-enzyme complexes with DD-peptidases. Deacylation of these complexes is very slow because the

† This research was supported in part by grants from the State of Connecticut Critical Technologies Program in Drug Design and the UConn Research Foundation (to J.A.K.) and from the National Institutes of Health (to R.F.P.).

* To whom correspondence should be addressed. E-mail: rpratt@wesleyan.edu. Tel: 860-685-2629. Fax: 860-685-2211 (R.F.P.); E-mail: judith.kelly@uconn.edu. Tel: 860-486-4353. Fax: 860-486-4331 (J.A.K.).

‡ University of Connecticut.

§ Wesleyan University.

[1] Abbreviations: DD-peptidase, D-alanyl-D-alanine carboxypeptidase/transpeptidase; E1′, covalent complex between **1** and the R61 peptidase; E4′, covalent complex of **4** with the peptidase; PBP, penicillin-binding protein.

10.1021/bi049612c CCC: $27.50
Published on Web 05/11/2004

Scheme 1

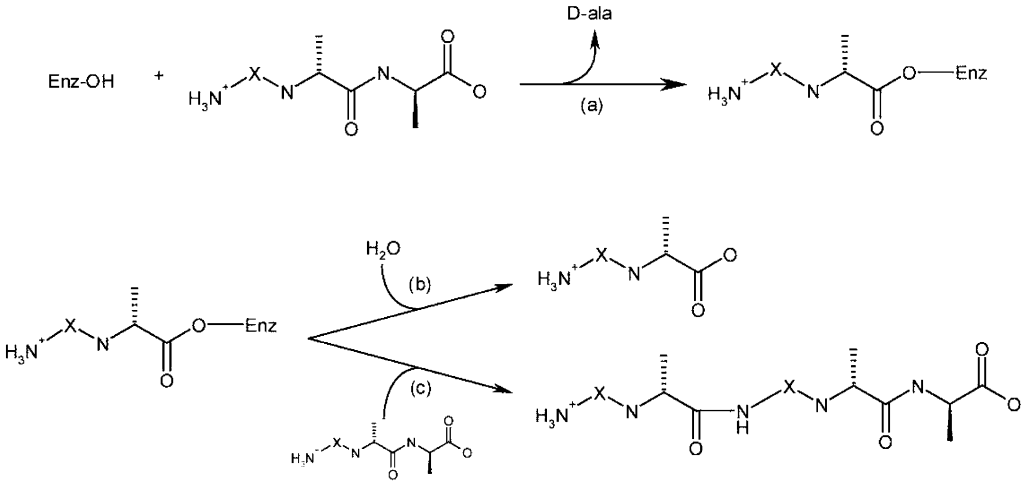

leaving group remains tethered near the ester of the acyl enzyme and blocks the approach of the deacylating nucleophile (the amino group of an acceptor molecule or a hydrolytic water molecule) (*8*−*10*).

The continued efficacy of β-lactams as therapeutic agents is seriously threatened by the constant evolution of resistance mechanisms by bacteria. The most immediate threat is posed by β-lactamases, enzymes that hydrolyze and inactivate β-lactams with startling efficiency. β-lactamases are acylated by β-lactams in the same manner as DD-peptidases. The resulting acyl enzyme, however, is quickly hydrolyzed by the enzyme (*11*−*16*). Drugs that inhibit both DD-peptidases and β-lactamases or that are at least resistant to β-lactamases are desperately needed to combat the resistant infections of today.

Cyclic acyl phosph(on)ates are one promising class of compounds shown to inhibit both β-lactamases and DD-peptidases (*17*−*19*). These compounds were designed to be penicillin-like inhibitors, in that they are cyclic, and therefore the "leaving group" might block access of the deacylating nucleophile (water) after their reaction with the enzyme. The inhibition is thought to follow the following mechanism:

$$E + I \rightleftharpoons EI \rightleftharpoons EI'$$

where EI represents a noncovalent enzyme−inhibitor complex and EI′, a covalent complex. Both the bicyclic phosphate **1** and its phosphonate analog **2** were shown to inhibit the class C β-lactamase of *Enterobacter cloacae* P99, as well as the *Streptomyces* strain R61 DD-peptidase, a 37.5-kDa exocellular enzyme that is a model for membrane-bound PBPs that catalyze the majority of cell-wall syntheses. However, the inhibition observed with these enzymes was reversible because the inhibitors themselves were found to slowly recyclize to reform the bicyclic compound (*17*, *18*). Product analysis indicated that these inhibitors phosph(on)-ylated the active-site serine of the β-lactamase. It has also been shown previously that the monocyclic acyl phosph(on)ates, **3**−**5**, inhibit the P99 β-lactamase and the class A TEM β-lactamase (*19*). The inhibition of the P99 enzyme by **4** is irreversible. It was speculated that this might reflect the additional degree of freedom available to **4** compared to the bicyclic phosphate **1** that allows the monocyclic inhibitor, after ring opening, to adopt a conformation that prevents the recyclization reaction. Product analysis and ^{31}P nuclear magnetic resonance spectra suggested that the inhibition of β-lactamases by monocyclic acyl phosphates involves acylation rather than phosphorylation of the active-site serine (*19*). We have now demonstrated that the monocyclic acyl phosphate **4** reversibly inactivates the R61 DD-peptidase.

Described here are the X-ray crystal structures of covalent complexes between the DD-peptidase and **1** (E1′) and **4** (E4′). These structures show that **1** and **4** interact with the peptidase active site in a unique way. These results, together with those from molecular modeling, suggest an explanation for the differences between the reactions of these cyclic phosph(on)ates with the R61 DD-peptidase and the P99 β-lactamase, an enzyme of very similar structure. Finally, these structures suggest new motifs that might be incorporated into the DD-peptidase inhibitor design.

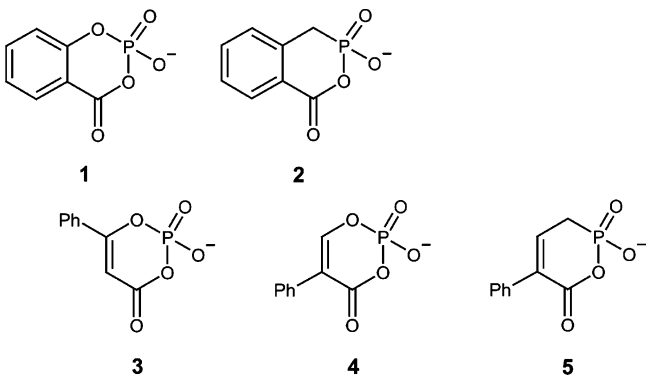

EXPERIMENTAL PROCEDURES

Enzyme Kinetics. Compounds **1** and **4** were prepared as previously described (*17*, *19*). The rate constant for inactivation of the R61 DD-peptidase by **4** was determined by monitoring the activity of a reaction mixture containing 100 μM **4** and 2 μM enzyme as a function of time against a depsipeptide substrate, *m*[[(phenylacetyl)glycyl]oxy]benzoic acid (*20*). All kinetic experiments were performed in a 20 mM MOPS buffer at pH 7.5 and 25 °C. Reactivation rates were obtained from the total progress curves generated by dilution of an enzyme/inhibitor incubation mixture into a substrate solution (*19*). Incubation mixtures contained 2.0 μM enzyme with 1.0 mM **1** or 0.1 mM **4**, and incubation periods were 2 h and 40 min, respectively. After these times,

Scheme 2

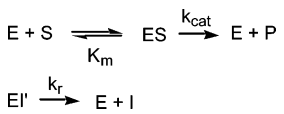

25-μL aliquots of the reaction mixtures were added to cuvettes containing solutions of the above-mentioned depsipeptide substrate (1 mL). Progress curves for substrate hydrolysis, monitored spectrophotometrically at 300 nm in the presence and absence of the inhibitor, were recorded. These data were fitted to Scheme 2 by means of Dynafit (*21*) to obtain the reactivation rate constant, k_r. In this scheme, EI′ represents the covalent complex of enzyme E with the inhibitor I, and S and ES represent the reporter substrate and its productive complex with the enzyme, repectively; the breakdown of EI′ is shown to regenerate I, as observed with the P99 β-lactamase (*18*).

Crystallization and Data Collection. Crystals of the R61 DD-peptidase were obtained using the hanging drop vapor diffusion method as described (*22*). To trap the R61−**1** complex, a 0.3 × 0.13 × 0.05-mm crystal was soaked for 5 h in a solution containing 30% poly(ethylene glycol) (PEG) 8000, 50 mM sodium phosphate at pH 6.8, 5% (w/v) glycerol, and ∼10 mM **1**. Cryprotection was accomplished by transferring the crystal into a fresh drop of the soak solution having 10% glycerol for 1 min and then into another drop having 20% glycerol. The crystal was then flash-cooled in a gaseous nitrogen stream at 100 K. Data were collected on Beamline X12C at the National Synchrotron Light Source (NSLS), Brookhaven National Laboratory, Upton, NY and processed using the HKL package (*23*). The R61−**4** complex was prepared in exactly the same way (crystal size = 0.78 × 0.4 × 0.2 mm), except the soak solution contained 5 mM **4**, and the soak time was 22.5 h. Data for the R61−**4** complex were collected on NSLS Beamline X12C (see Table 1).

Crystallographic Structure Refinement. Initial refinement of both structures was done using CNS (*24*) at a 1.5 Å resolution. Solvent molecules with reasonable hydrogen-bond distances and geometries were added. Care was taken to avoid modeling the density for the bound inhibitors as solvent. Once the refinements converged (R_{cryst} = 18.5 and R_{free} = 21.0 for E1′; R_{cryst} = 17.9 and R_{free} = 19.7 for E4′), further refinement was done using SHELX-97 (*25*). After isotropic refinement at full resolution, both models were refined anisotropically. Refinement of the individual anisotropic displacement parameters resulted in a 2.9% drop in R_{free} for E1′ and 1.2% for E4′, with comparable drops in R_{cryst}. Iterative cycles of fitting in XtalView (*26*) followed by refinement in SHELXL continued until the *R* factors converged at 11.5% (R_{free} = 15.1%) and 11.0% (R_{free} = 14.5%) for E1′ and E4′, respectively. At this point, those hydrogen atoms visible as 3σ peaks in $|F_o| - |F_c|$ electron density maps and with good geometry were added using the riding model in SHELXL. Adding hydrogen atoms resulted in an almost 1% drop in the *R* factors.

Molecular Modeling. Molecular modeling was performed using InsightII 2000 software (MSI, San Diego, CA), running on an SGI Octane 2 computer. The protein structures selected for docking were those of the phosphonate complexes of the P99 β-lactamase (PDB 1BLS; ref *27*) and the R61 DD-peptidase (PDB 1MPL; ref *28*). The active-site residues in these structures would presumably be in the "active" conformation. A model of **4** was constructed by means of the Builder module of InsightII and subjected to energy minimization. It was then visually docked into the active sites according to the following criteria. For the "prephosphorylation" complexes, the P atom was placed at a distance of less than 3 Å from Ser O_γ of the active site, where the Ser O_γ −P−OCO angle was 180°, appropriate for a direct "in-line" displacement at phosphorus. One of the P−O^- oxygens was then placed at a distance <3 Å from the backbone nitrogen atoms of the oxyanion hole (Thr301 and Ser62 in the case of the DD-peptidase and Ser318 and Ser64 for the β-lactamase). These restrictions yielded two alternative orientations of the ligand with respect to the protein,

Table 1: Crystallographic Data

	E1′	E4′
resolution limit (Å)	1.15	1.13
number of reflections		
measured	780 703	1 385 496
unique	119 308	120 972
(reflections, $F > 4\sigma$)	102 281	114 325
completeness (%)		
all data	97.7	94.1
highest resolution shell	82.9 (1.19−1.15 Å)	70.8 (1.17−1.13 Å)
R_{sym}[a] (on *I*)	0.056	0.062
[$I/\sigma(I)$]		
overall	28.8	29.9
highest resolution shell	4.3	17.3
refinement		
resolution (Å)	10−1.15	10 − 1.13
R_{cryst} (all data)	0.107	0.104
R_{free}	0.140	0.144
data in test set	5813	2737
non-hydrogen atoms	3210	3289
rms deviations		
bond lengths (Å)	0.079	0.030
angles (deg)	2.25	1.742
average *B* factor (all atoms) (Å^2)	9.1	8.9
average *B* factor of ligand (Å^2)	15.3	11.4

[a] $R_{sym} = \Sigma|I_{obs} - (I)|/\Sigma(I)$.

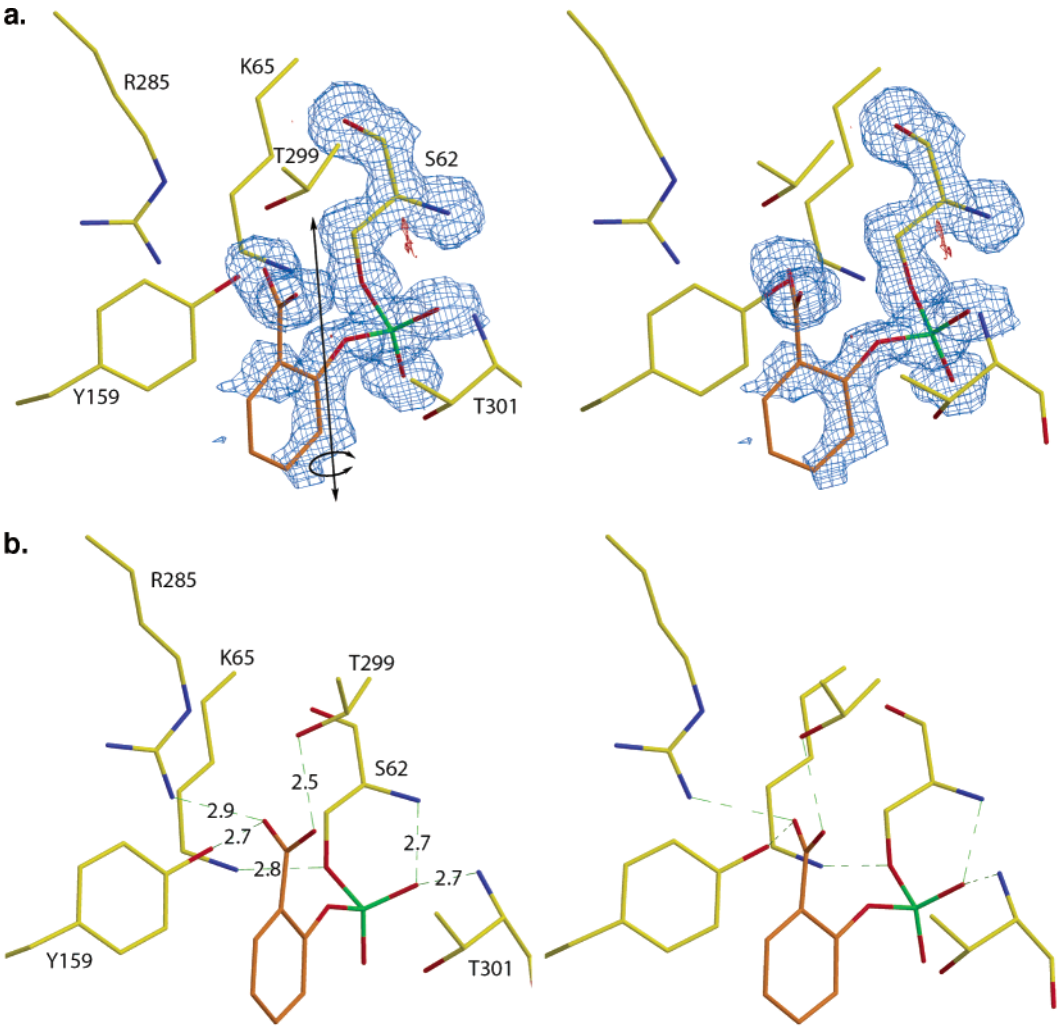

FIGURE 1: Stereoview of the E1′ complex (a) showing $2|F_o| - |F_c|$ electron density contoured at 1.5σ (blue mesh), as well as $|F_o| - |F_c|$ density contoured at 3.0σ (green mesh) and -3.0σ (red mesh). The black arrows indicate the axis of oscillation of compound **1**. Note the lack of density for the distal portion of the ring and the smearing of the density for the oxygen atom connecting the ring to the phosphorus. There is also no positive (green) difference density, indicating that the parts of the model lacking density are not simply misfit. A similar view without electron density (b) shows the contacts between **1** and the R61 active site. Both images were rendered using XtalView and RASTER3D (*26*, *39*).

depending on which P−O$^-$ was placed in the oxyanion hole. For the "preacylation" complexes, the carbonyl carbon of **4** was placed <3 Å from the active-site Ser O_γ, where the Ser O_γ−C═O angle was 120°, appropriate for nucleophilic attack at a carbonyl group. The carbonyl oxygen was also placed in the oxyanion hole. This procedure also yields two orientations where nucleophilic attack is on either the *si* or *re* face of the carbonyl.

RESULTS AND DISCUSSION

The monocyclic acyl phosphate 1-hydroxy-4-phenyl-2,6-dioxaphosphorinanone(3)-1-oxide (**4**), like 1-hydroxy-4,5-benzo-2,6-dioxaphosphorinanone (3)-1-oxide (**1**), inactivates the R61 DD-peptidase. The second-order rate constants of inactivation by **1** and **4** were 0.46 (*17*) and 24 s^{-1} M^{-1}, respectively. These reactions are much slower than those with the structurally similar *E. cloacae* P99 β-lactamase (*17*, *19*), which is usual with nonspecific reagents. The inactivation of the DD-peptidase by **1** and **4** is slowly reversible, with rate constants for reactivation of $(2.7 \pm 0.5) \times 10^{-5}$ s^{-1} and $(8.9 \pm 0.6) \times 10^{-5}$ s^{-1}, respectively. The structures of these quite inert complexes were of interest because these may indicate how novel inhibitory entities may occupy the active site. Of particular interest was the question of whether **1** and **4** inhibited the peptidase by acylation or phosphorylation.

We have determined the X-ray crystal structures of the two inhibitors, **1** and **4**, in the complexes with the R61 DD-peptidase at a 1.1 Å resolution. The models have been refined to crystallographic *R* factors of 10.7 and 10.4%, respectively, for all data (Table 1, PDB 1SDE and 1SCW). The structures clearly indicate the mode of inhibition (acylation versus phosphorylation) and explain several curious differences observed in the reactions of **1** and **4** with the R61 DD-peptidase and the P99 class C β-lactamase.

E1′ Complex. The *Streptomyces* R61 DD-peptidase is preferentially phosphorylated by the bicyclic phosphate **1** on the time scale of this crystallographic experiment. The binding mode of **1** is unlike any other molecule studied crystallographically with this enzyme. The active site of the DD-peptidase is a deep channel leading to the catalytic Ser62. The top of the active-site pocket has a significant positive charge (*29*) primarily because of Arg285. Normally, the substrates (*30*) and inhibitors (*28*, *31*) lay along the active-site channel. Specific ligands commonly bind with a side-

Scheme 3

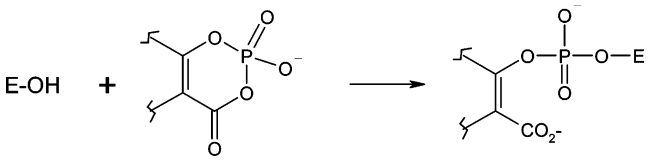

chain amide interacting with the carbonyl of Thr301, a carbonyl interacting with the side chain of Asn161, and an oxygen atom bound in the oxyanion hole formed by the main-chain amides of Ser62 and Thr301. Negative charges, such as the carboxylate of the terminal D-Ala residue of the natural cell-wall substrate or the C3 carboxylate of penicillins, often form salt bridges with Arg285 (*30*−*32*). A hydrophobic surface on the back of the active site interacts with the nonpolar groups of many ligands. The methylene portion of the diaminopimelate of the natural cell-wall peptide, for example, lies across this hydrophobic surface. Finally, in the case of the natural cell-wall peptide, a subsite of the active site has evolved to recognize the glycyl-diaminopimelate moiety of the substrate. Unlike other inhibitors and substrates, **1** interacts only with the oxyanion hole, Arg285, and Thr299, while the bulk of the molecule protrudes from the active site.

The continuous density between the phosphorus of the inhibitor and Ser62 O_γ indicates that the two are indeed covalently bound (Figure 1a). The inhibition reaction is therefore that shown in Scheme 3.

One of the phosphoryl oxygens is bound in the oxyanion hole (2.7 Å from both Ser62 and Thr301 amides; Figure 1b). This causes the other phosphoryl oxygen anion to project into the active site, while the oxygen that bears the phenyl ring and the newly formed carboxylate points out of the active site past Tyr159. The carboxylate interacts with both Arg285 (2.9 Å) and Thr299 (2.5 Å). The phenyl ring of **1** is not in a position to interact with the ring of Tyr159. Given the relatively small number of interactions compared to other inhibitors, it is apparent that the E1′ complex is not well-stabilized by the enzyme. The paucity of strong interactions with the enzyme is evident in the high *B* factors (Figure 3a) and incomplete electron density for a portion of the phenyl ring (Figure 1a). Indeed, the inhibitor appears to be oscillating slightly about the axis shown in Figure 1a. Such a movement would account for the appearance of the observed electron density.

E4′ Complex. As we saw with **1**, the R61 enzyme is also preferentially phosphorylated (Scheme 3) rather than acylated by **4** over the time scale of these experiments. Again, the covalent nature of the inhibitory complex is indicated by the continuous electron density between the inhibitor phosphorus and Ser62 O_γ (Figure 2a). There is no suggestion of any acylated enzyme in the difference electron density map. In

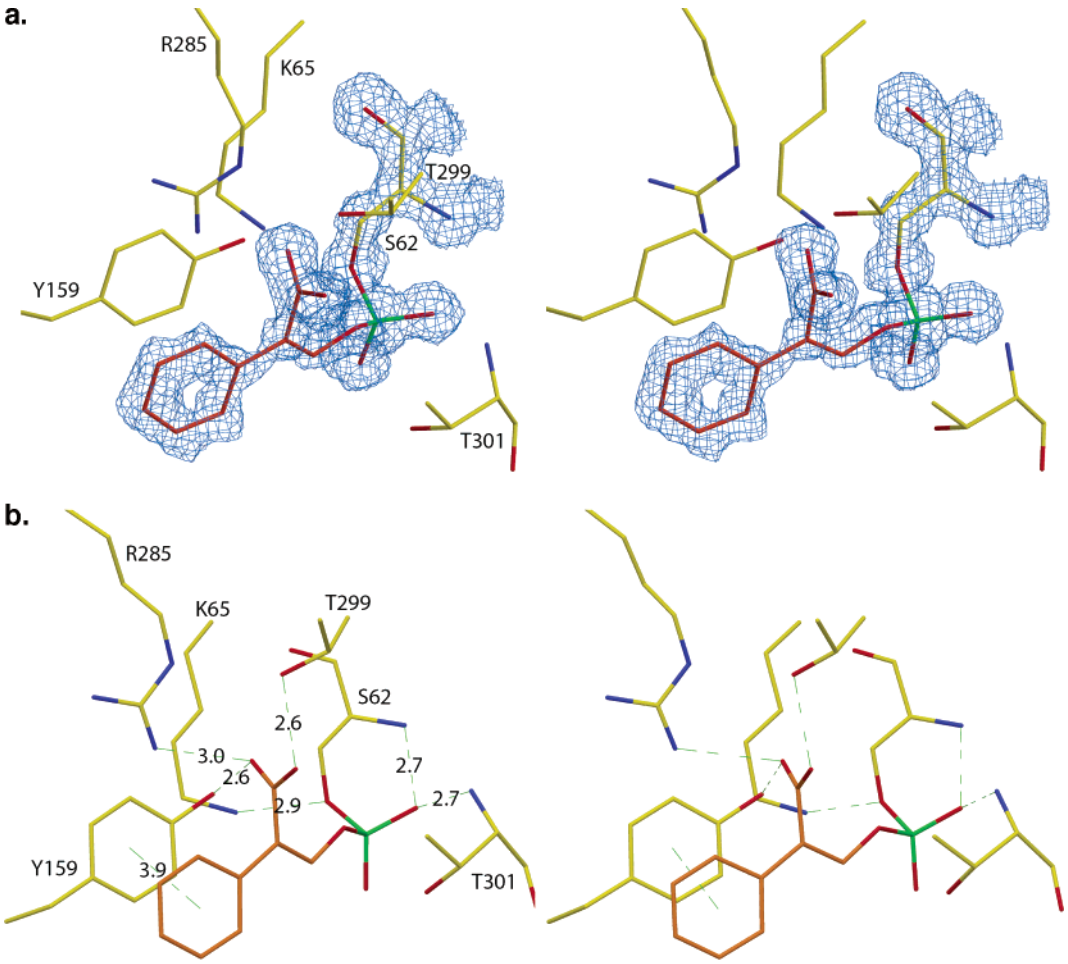

FIGURE 2: Stereoview of the E4′ complex (a) showing $2|F_o| - |F_c|$ electron density contoured at 1.5σ (blue mesh), as well as $|F_o| - |F_c|$ density contoured at 3.0σ (green mesh) and -3.0σ (red mesh). The density is well-defined for the entire inhibitor, and there is no difference density in the vicinity. A similar view without electron density (b) shows the contacts between **4** and the active site. Both images were rendered using XtalView and RASTER3D.

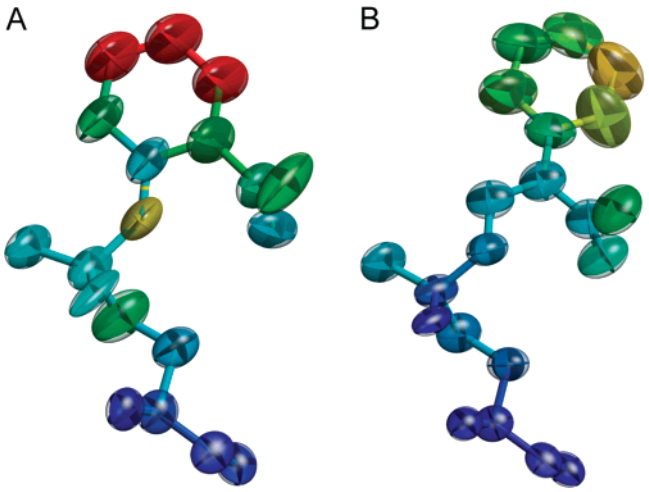

FIGURE 3: Views of the thermal ellipsoids of **1** (a) and **4** (b). Atoms are colored by the temperature factor, with dark blue representing a *B* factor of 10 Å^2 or less and red representing a *B* factor of 25 Å^2 or greater. The shapes of the thermal ellipsoids correspond to the direction and magnitudes of the anisotropic displacement parameters. Images were prepared using RASTEP (*39*).

contrast, the P99 β-lactamase was found to be preferentially acylated by **4** (*19*). In the current structure, the monocyclic phosphate **4** is bound in a fashion remarkably similar to **1**, with the ring structure projecting out of the active-site pocket near Tyr159. A phosphoryl oxygen is bound in the oxyanion hole (2.7 Å from both Ser62 and Thr301 main-chain amides; Figure 2b). In both the E1′ and E4′ complexes, one phosphoryl oxygen is directed into the active-site pocket of the enzyme. This is a unique observation for phosphyl derivatives of both this enzyme and of the class C β-lactamases. The oxygen atom in question, which must bear a significant negative charge, is not hydrogen-bonded to any residue of the protein. Its major local interaction with the protein would appear to be with the positively charged terminus of Lys65 (the O−N distances are 4.4 and 4.5 Å for **1** and **4**, respectively). In addition, it does accept hydrogen bonds from three solvent molecules that occupy the active site in the region where the side chain of a normal substrate would bind. The carboxylate group interacts with both Arg285 (3.0 Å) and Thr299 (2.6 Å). Interestingly, the extra length of **4** allows it to make an interaction with the enzyme that is not available to **1**. The phenyl ring of the monocyclic phosphate is in a position to interact with the ring of Tyr159 (3.9 Å between the ring centers). The two rings are nearly parallel, with the edge of one ring positioned over the center of the other. This single additional interaction is apparently enough to stabilize the E4′ complex. The *B* factors and thermal ellipsoids are significantly smaller for this structure than for E1′ (Figure 3b). The average *B* factor of **4** is 11.4 Å^2, compared to 15.3 Å^2 for **1** in the E1′ complex. Also, the electron density for E4′ is well-defined for the entire inhibitor (Figure 2a).

It had been thought that the extra degree of freedom inherent in **4** might allow it to take on a different conformation from that of **1** and thus eliminate the recylization reaction (*18*). Instead, both inhibitors adopt nearly identical conformations (Figures 1b and 2b). The reactivation rates are therefore not very different although the rate for the complex of **1** is rather smaller than that for **4** (see the Results). This difference may reflect steric problems with the more-rigid ligand derived from **1** associated with the reorientation required for the recyclization that probably accompanies reactivation of the enzyme (*18*).

*Molecular Modeling of **4** in Complexes with the R61 DD-Peptidase and P99 β-Lactamase.* Molecular modeling was employed to gain an understanding of the structural basis for the products observed. Intact compound **4** was manually docked into the active site of the R61 DD-peptidase and the P99 β-lactamase in the orientations required for acylation on one hand and phosphorylation on the other hand (see the Experimental Procedures). Figure 4 shows one possible structure of the noncovalent prephosphorylation complex of **4** with the DD-peptidase. It can be seen that there are no unfavorable steric interactions between the inhibitor and any residue of the active site. The Ser62 hydroxyl group (aided perhaps by the attendant Lys65 and/or Tyr159) is poised to attack the phosphorus atom of the inhibitor in such a way that the carboxylate leaving group is positioned in an appropriately in-line fashion. One of the phosphoryl oxygens is similarly poised to enter the oxyanion hole (backbone NH groups of Ser62 and Thr301). The alternative orientation for in-line attack (not shown; see the Experimental Procedures)

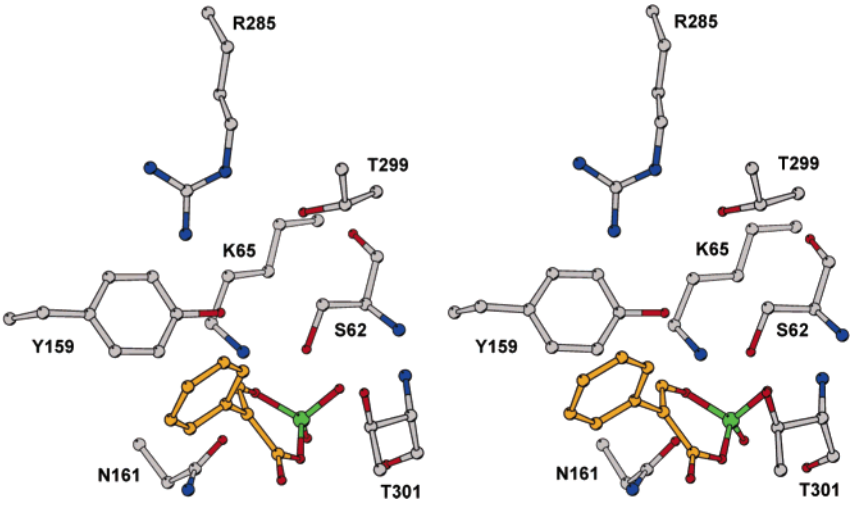

FIGURE 4: Stereoview of the modeled prephosphorylation complex between **4** and the R61 DD-peptidase. The carbon atoms of the inhibitor are colored orange, while those of the enzyme are colored gray. The figure was rendered using MOLSCRIPT (*40*).

seems less favorable because the phenyl group is directed more deeply into the protein where it would contact Asn161, for example.

Acylation complexes of **4** with the peptidase do indeed look less favorable. In one orientation, the phenyl and phosphoryl groups would closely contact the β3 strand (as defined in ref *29*) and Asn161, respectively. In the alternative orientation, where the opposite face of the carbonyl is presented to Ser62 O_γ, the phenyl and phosphoryl groups would probably be unacceptably close to Trp233 and Tyr159, respectively. These unfavorable steric clashes in the preacylation complexes, in contrast to the apparently unimpeded prephosphorylation complex of Figure 4, may explain why **4** phosphorylates rather than acylates the active site. A similar explanation would also likely apply to **1**.

It is interesting to compare the models described above with the situation in the P99 β-lactamase where the enzyme appears to be acylated rather than phosphorylated (*19*). In this case, docking models suggest that the prephosphorylation complex would be sterically disfavored. In particular, it is clear that in one such complex, the phenyl group of **4** would directly impact the H10a loop (residues 289−292) that hovers above the active site (*33*). This loop, not present in the R61 DD-peptidase, is thought to close off the extended substrate-binding site of the DD-peptidase, a necessary step in β-lactamase evolution (*34*, *35*). The interaction of β-lactams with this loop is known to influence the specificity of class C β-lactamases (*36*). The alternative prephosphorylation orientation also appears unfavorable; in this case, the phenyl ring closely approaches Tyr221, another important factor in β-lactamase evolution (*20*). In contrast, at least one of the preacylation complexes of **4** with the P99 β-lactamase looks competent. Here, the phenyl ring seems to comfortably occupy the side-chain-binding site adjacent to the β3 strand. Thus, acylation, rather than phosphorylation, may be the poison favored by the β-lactamase. It may be noted here that, although the active-site components of the DD-peptidase and β-lactamase are very similar, the general shapes of the active sites are significantly different (*20*). Thus, it is not surprising that nonspecific molecules may interact with them differently.

CONCLUSIONS

Cyclic acyl phosphates are versatile, bifunctional reagents that can inactivate enzymes by either acylation or phosphorylation. Competition between these modes of reaction has also been observed with acyclic analogues of **4** (*37*). Elements of the crystal structures of **1** and **4** bound to the DD-peptidase will be relevant to further inhibitor design. Although the positions of the phosphoryl oxygen in the oxyanion hole and the carboxylate interacting with Tyr159 (presumably protonated), Arg285, and Thr299 are common to substrates and substratelike ligands, those of the phenyl ring and the other phosphoryl oxygen are novel. These motifs should certainly be considered in further design although, with respect to the R61 DD-peptidase, at least a more-efficient delivery vehicle (more specific interactions with active-site residues) would have to be used. Extension of the aromatic ring into the β-lactam side-chain binding site might prove effective, for example, because this enzyme is extremely receptive to a specific side chain (*38*).

ACKNOWLEDGMENT

We acknowledge Jean-Marie Frère at Université of Liège for providing the R61 enzyme and Robert Sweet, Anand Saxena, and the staff at Brookhaven National Laboratory, National Synchrotron Light Source, Beamline X12C (supported by the U.S. Department of Energy, Division of Materials Sciences and Division of Chemical Sciences, under contract DE-AC02-98CH10886) for help in data collection.

REFERENCES

1. Spratt, B. G. (1994) in *Bacterial Cell Wall* (Ghuysen, J.-M., and Hakenbeck, R., Eds.) pp 517−534, Elsevier, Amsterdam, The Netherlands.
2. Walsh, C. T. (1989) Enzymes in the D-alanine branch of bacterial cell wall peptidoglycan assembly, *J. Biol. Chem. 264*, 2393−2396.
3. Bugg, T. D., and Walsh, C. T. (1992) Intracellular steps of bacterial cell wall peptidoglycan biosynthesis: enzymology, antibiotics, and antibiotic resistance, *Nat. Prod. Rep. 9*, 199−215.
4. Ghuysen, J. M., Charlier, P., Coyette, J., Duez, C., Fonze, E., Fraipont, C., Goffin, C., Joris, B., and Nguyen-Distèche, M. (1996) Penicillin and beyond: evolution, protein fold, multimodular polypeptides, and multiprotein complexes, *Microb. Drug Resist. 2*, 163−175.
5. Frère, J. M., and Joris, B. (1985) Penicillin-sensitive enzymes in peptidoglycan biosynthesis, *CRC Crit. Rev. Microbiol. 11*, 299−396.
6. Koch, A. L. (2000) Penicillin binding proteins, β-lactams, and β-lactamases: offensives, attacks, and defensive countermeasures, *Crit. Rev. Microbiol. 26*, 205−220.
7. Pratt, R. F. (2002) Functional evolution of the serine β-lactamase active site, *J. Chem. Soc., Perkin Trans. 2*, 851−861.
8. Waxman, D. J., and Strominger, J. L. (1983) Penicillin-binding proteins and the mechanism of action of β-lactam antibiotics, *Annu. Rev. Biochem. 52*, 825−869.
9. Tipper, D. J., and Strominger, J. L. (1965) Mechanism of action of penicillins: a proposal based on their structural similarity to acyl-D-alanyl-D-alanine, *Proc. Natl. Acad. Sci. U.S.A. 54*, 1133−1141.
10. Tipper, D. J. (1985) Mode of action of β-lactam antibiotics, *Pharmacol. Ther. 27*, 1−35.
11. Kelly, J. A., Dideberg, O., Charlier, P., Wery, J.-P., Libert, M., Moews, P. C., Knox, J. R., Duez, C., Fraipont, C., Joris, B., Dusart, J., Frère, J.-M., and Ghuysen, J.-M. (1986) On the origin of bacterial resistance to penicillin: Comparison of a β-lactamase and a penicillin target, *Science 231*, 1429−1431.
12. Knowles, J. R. (1985) Penicillin resistance: the chemistry of β-lactamase inhibition, *Acc. Chem. Res. 18*, 97−104.
13. Frère, J. M., and Joris, B. (1988) β-lactamases as the main resistance factor to penicillin-related antibiotics, *Ann. Biol. Clin. 46*, 151−156.
14. Reading, C., and Farmer, T. (1981) Inhibition of β-lactamases from Gram-negative bacteria by clavulanic acid, *Biochem. J. 199*, 779−787.
15. Bush, K. (1989) Characterization of β-lactamases, *Antimicrob. Agents Chemother. 33*, 259−263.
16. Waley, S. G. (1992) in *The Chemistry of β-Lactams* (Page, M. I., Ed.) pp 198−228, Blackie Academic & Professional, London, U.K.
17. Pratt, R. F., and Hammar, N. J. (1998) Salicyloyl cyclic phosphate, a "penicillin-like" inhibitor of β-lactamases, *J. Am. Chem. Soc. 120*, 3004−3006.
18. Kaur, K., Lan, M. J., and Pratt, R. F. (2001) Mechanism of Inhibition of the Class C β-Lactamase of *Enterobacter cloacae* P99 by Cyclic Acyl Phosph(on)ates: Rescue by Return, *J. Am. Chem. Soc. 123*, 10436−10443.
19. Kaur, K., Adediran, S. A., Lan, M. J., and Pratt, R. F. (2003) Inhibition of β-lactamases by monocyclic acyl phosph(on)ates, *Biochemistry 42*, 1529−1536.
20. Bernstein, N. J., and Pratt, R. (1999) On the importance of a methyl group in β-lactamase evolution: Free energy profiles and molecular modeling, *Biochemistry 38*, 10499−10510.
21. Kuzmic, P. (1996) Program DYNAFIT for the analysis of enzyme kinetic data: application to HIV proteinase, *Anal. Biochem. 237*, 260−273.

22. Kelly, J. A., Knox, J. R., Zhao, H., Frère, J.-M., and Ghuysen, J.-M. (1989) Crystallographic mapping of β-lactams bound to a DD-peptidase, *J. Mol. Biol. 209*, 281−295.
23. Otwinowski, Z., and Minor, W. (1997) Processing of X-ray diffraction data collected in oscillation mode, *Methods Enzymol. 276*, 307−326.
24. Brunger, A. T., Adams, P. D., Clore, G. M., DeLano, W. L., Gros, P., Grosse-Kunstleve, R. W., Jiang, J. S., Kuszewski, J., Nilges, M., Pannu, N. S., Read, R. J., Rice, L. M., Simonson, T., and Warren, G. L. (1998) Crystallography & NMR system: A new software suite for macromolecular structure determination, *Acta Crystallogr., Sect. D 54*, 905−921.
25. Sheldrick, G. M., and Schneider, T. R. (1997) SHELXL: high-resolution refinement, *Methods Enzymol. 277*, 319−343.
26. McRee, D. E. (1999) XtalView/Xfit- -A versatile program for manipulating atomic coordinates and electron density, *J. Struct. Biol. 125*, 156−165.
27. Lobkovsky, E., Billings, E. M., Moews, P. C., Rahil, J., Pratt, R. F., and Knox, J. R. (1994) Crystallographic structure of a phosphonate derivative of the *Enterobacter cloacae* P99 cephalosporinase: Mechanistic interpretation of a β-lactamase transition-state analogue, *Biochemistry 33*, 6762−6772.
28. Silvaggi, N. R., Anderson, J. W., Brinsmade, S. R., Pratt, R. F., Kelly, J. A. (2003) Crystal Structure of Phosphonate-Inhibited D-Ala-D-Ala Peptidase Reveals an Analogue of a Tetrahedral Transition State, *Biochemistry 42*, 1199−1208.
29. Kelly, J. A., and Kuzin, A. P. (1995) Refined crystallographic structure of a DD-peptidase penicillin target enzyme at 1.6 Å resolution, *J. Mol. Biol. 254*, 223−236.
30. McDonough, M., Anderson, J., Silvaggi, N., Pratt, R., Knox, J., and Kelly, J. (2002) Structures of Two Kinetic Intermediates Reveal Species Specificity of Penicillin-Binding Proteins, *J. Mol. Biol. 322*, 111.
31. Kuzin, A. P., Liu, H., Kelly, J. A., and Knox, J. R. (1995) Binding of cephalothin and cefotaxime to D-ala-D-ala peptidase reveals a functional basis of a natural mutation in a low-affinity penicillin-binding protein and in extended-spectrum β-lactamases, *Biochemistry 34*, 9532−9540.
32. Lee, W., McDonough, M. A., Kotra, L. P., Li, Z. H., Silvaggi, N. R., Takeda, Y., Kelly, J. A., and Mobashery, S. (2001) A 1.2 Å snapshot of the final step of bacterial cell wall biosynthesis, *Proc. Natl. Acad. Sci. U.S.A. 98*, 1427−1431.
33. Lobkovsky, E., Moews, P. C., Liu, H., Zhao, H., Frère, J.-M., and Knox, J. R. (1993) Evolution of an enzyme activity: Crystallographic structure at 2 Å resolution of the cephalosporinase from the *ampC* gene of *Enterobacter cloacae* P99 and comparison with a class A penicillinase, *Proc. Natl. Acad. Sci. U.S.A. 90*, 11257−11261.
34. Meroueh, S. O., Minasov, G., Lee, W., Shoichet, B. K., and Mobashery, S. (2003) Structural aspects for evolution of β-lactamases from penicillin-binding proteins, *J. Am. Chem. Soc. 125*, 9612−9618.
35. Massova, I., and Mobashery, S. (1998) Kinship and diversification of bacterial penicillin-binding proteins and β-lactamases, *Antimicrob. Agents Chemother. 42*, 1−17.
36. Nugaka, M., Haruta, S., Tanimoto, K., Kogure, K., Taniguchi, K., Tamaki, M., and Sawai, T. (1995) Molecular evolution of a class C β-lactamase extending its substrate specificity, *J. Biol. Chem. 270*, 5729−5735.
37. Kaur, K., and Pratt, R. F. (2001) Mechanism of reaction of acyl phosph(on)ates with the β-lactamase of *Enterobacter cloacae* P99, *Biochemistry 40*, 4610−4621.
38. Anderson, J. W., and Pratt, R. F. (2000) Dipeptide binding to the extended active site of the *Streptomyces* R61 D-alanyl-D-alanine peptidase: The path to a specific substrate, *Biochemistry 39*, 12200−12209.
39. Merrit, E. A., and Bacon, D. J. (1997) Raster3D: Photorealistic molecular graphics, *Methods Enzymol. 277*, 505−524.
40. Kraulis, P. (1991) MOLSCRIPT: a program to produce both detailed and schematic plots of protein structures, *J. Appl. Crystallogr. 24*, 946−950.

BI049612C